



저작자표시-비영리-변경금지 2.0 대한민국

이용자는 아래의 조건을 따르는 경우에 한하여 자유롭게

- 이 저작물을 복제, 배포, 전송, 전시, 공연 및 방송할 수 있습니다.

다음과 같은 조건을 따라야 합니다:



저작자표시. 귀하는 원저작자를 표시하여야 합니다.



비영리. 귀하는 이 저작물을 영리 목적으로 이용할 수 없습니다.



변경금지. 귀하는 이 저작물을 개작, 변형 또는 가공할 수 없습니다.

- 귀하는, 이 저작물의 재이용이나 배포의 경우, 이 저작물에 적용된 이용허락조건을 명확하게 나타내어야 합니다.
- 저작권자로부터 별도의 허가를 받으면 이러한 조건들은 적용되지 않습니다.

저작권법에 따른 이용자의 권리는 위의 내용에 의하여 영향을 받지 않습니다.

이것은 [이용허락규약\(Legal Code\)](#)을 이해하기 쉽게 요약한 것입니다.

[Disclaimer](#)

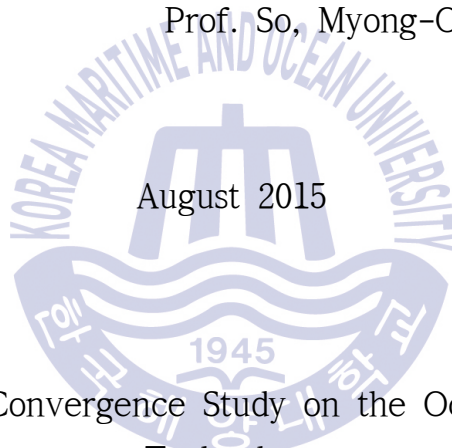
Thesis for Master Degree

Temperature Control of a CSTR Using a Nonlinear PID Controller

Advisor: Prof. Jin, Gang-Gyoo

Prof. So, Myong-Ok

August 2015



Department of Convergence Study on the Ocean Science and
Technology

School of Ocean Science and Technology
Korea Maritime and Ocean University

Lee, Joo-Yeon

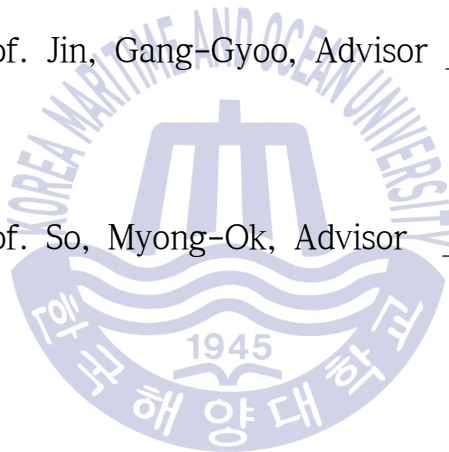
Approved by the Committee of the Ocean Science and Technology
School of Korea Maritime and Ocean University in Fulfillment of
the Requirements for the Degree of Master's in Engineering

Dissertation Committee :

Prof. Kim, Jong-Hwa, Chair _____

Prof. Jin, Gang-Gyoo, Advisor _____

Prof. So, Myong-Ok, Advisor _____



August 2015

Department of Convergence Study on the Ocean Science and Technology
Ocean Science and Technology School
Korea Maritime and Ocean University

ABSTRACT

Continuous stirred tank reactor (CSTR) which plays a key role in the chemical plants exhibits highly nonlinear behavior as well as time-varying characteristics during operation. So, CSTR process control over the whole operating range has been a challenging issue especially for control engineers. A variety of feedback control algorithms and their tuning methods have been developed to guarantee the satisfactory performance despite the varied dynamic characteristics of CSTRs.

This thesis presents a scheme of designing a nonlinear PID controller incorporating with a real-coded genetic algorithm (RCGA) for the temperature control of a CSTR process. The gains of the NPID controller are composed of easily implementable nonlinear functions based on the error and/or the error rate and its parameters are tuned using the RCGA by minimizing the integral of time-weighted absolute error (ITAE).

A set of simulation works for reference tracking and disturbance rejecting performances and robustness to parameter changes are carried out to compare with two other nonlinear controllers and show the feasibility of the proposed method.

Contents

Abstract	i
List of Tables	iv
List of Figures	v
Chapter 1. Introduction	
1.1 Background and Purpose	1
1.2 Method and Organization	2
Chapter 2. Continuous Stirred Tank Reactor	
2.1 Process Description	4
2.2 Analysis of the process	7
Chapter 3. Existing Controllers	
3.1 Linear PID Controller	9
3.1.1 Structure of linear PID controller	9
3.1.2 Role of LPID control action	10
3.1.3 Ziegler-Nichols (Z-N) tuning rules	11
3.2 Nonlinear PID Controller	15
3.2.1 Korkmaz' s NPID controller	16
3.2.2 Chen' s adaptive controller	18
Chapter 4. Proposed NPID Controller	
4.1 Structure of the Proposed NPID Controller	21
4.2 Gain of NPID Controller	22
4.2.1 Nonlinear proportional gain	22
4.2.2 Nonlinear integral gain	24
4.2.3 Nonlinear derivative gain	25
4.3 Tuning of the NPID Controller Parameters	26

Chapter 5. Simulation and Review

- 5.1 Parameters for Simulation and Controller Tuning..... 28
 - 5.1.1 Parameters for Simulation..... 28
 - 5.1.2 NPID controller tuning 28
- 5.2 Simulation and Performance Comparison 30
 - 5.2.1 Set-point tracking performance 30
 - 5.2.2 Disturbance rejection performance 34
 - 5.2.3 Robustness to parameter change 37
 - 5.2.4 Comparison of computing time 42

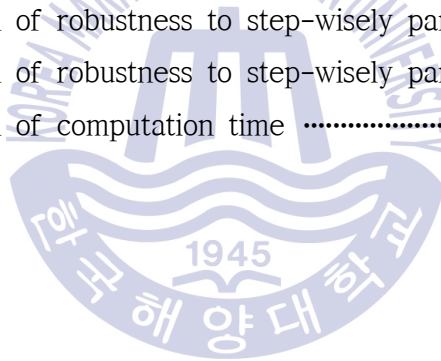
Chapter 6. Conclusion 44

References 45



List of Tables

Table 3.1 PID tuning rules by the open-loop method	13
Table 3.2 Tuning rules by the closed-loop method	15
Table 5.1 Tuned parameters of the proposed NPID controller and Korkmaz' s controller	29
Table 5.2 Comparison of set-point tracking performances when y_r is step-wisely increased from 0.886 to 4.705	32
Table 5.3 Comparison of set-point tracking performances when y_r is decreased from 4.705 to 0.886	34
Table 5.4 Comparison of disturbance rejection performances when d_1 and d_2 are step-wisely changed	37
Table 5.5 Comparison of robustness to step-wisely parameter changes ·	42
Table 5.6 Comparison of robustness to step-wisely parameter changes ·	42
Table 5.7 Comparison of computation time	43



List of Figures

Fig. 2.1 Nonisothermal CSTR process	5
Fig. 2.2 Block diagram of the CSTR process with a saturator	7
Fig. 2.3 Phase-portrait for three equilibrium points	8
Fig. 2.4 Step responses of the CSTR	8
Fig. 3.1 Structure of the standard LPID controller	10
Fig. 3.2 Example of three control actions of the LPID controller	11
Fig. 3.3 Step response of a process	12
Fig. 3.4 Closed-loop control system with a proportional gain	14
Fig. 3.5 Response curve and ultimate period	14
Fig. 3.6 Gaussian error function	17
Fig. 3.7 Nonlinear gain functions proposed by Korkmaz et al.	18
Fig. 3.8 Adaptive control system proposed by Chen and Peng	19
Fig. 3.9 Significance of $\tilde{u}(t)$ to the changes of $m(\theta=0)$	20
Fig. 4.1 Structure of the proposed NPID controller	22
Fig. 4.2 $K_p(e)$ shapes to changes of $e(a_1 = 2, a_2 = 1)$	23
Fig. 4.3 $K_i(e)$ shapes to changes of $e(b = 1)$	24
Fig. 4.4 $K_d(e, \dot{e})$ shapes to changes of $e(c_1 = c_2 = 1)$	26
Fig. 4.5 Tuning of the proposed NPID controller with a saturator	26
Fig. 5.1 Changing the set-point for parameter tuning	29
Fig. 5.2 Set-point tracking responses when $y_r(t)$ is step-wisely increased from 0.886 to 4.705	31
Fig. 5.3 Set-point tracking responses when y_r is step-wisely decreased from 4.705 to 0.886	33
Fig. 5.4 Disturbance rejection responses when d_1 and d_2 are step-wisely changed while $y_r = 2.75(d_1 = d_2 = 0.2)$	35

Fig. 5.5 Disturbance rejection responses when d_1 and d_2 are step-wisely
 changed while $y_r = 2.75(d_1 = -0.2, d_2 = 0.2)$ 36

Fig. 5.6 Response comparison to parameter changes($D_a = 0.072 \rightarrow 0.09$) 38

Fig. 5.7 Response comparison to parameter changes($D_a = 0.072 \rightarrow 0.05$) 39

Fig. 5.8 Response comparison to parameter changes($D_a = 0.09, H = 9$) .. 40

Fig. 5.9 Response comparison to parameter changes($D_a = 0.05, H = 7$) .. 41



Chapter 1. Introduction

1.1. Background and Purpose

Chemical reactors have been using to produce the reaction and playing a major role in the petrochemical industry. Chemical reactors can be divided into two categories, batch type and continuous type, according to their type and size. Continuous stirred tank reactors (CSTRs) can be considered as a representative of continuous type reactor. Since chemical reaction occurring in the CSTR is greatly affected by concentration of the reactants, temperature, pressure, catalyst and time, they show significant nonlinear and time-varying characteristics, that is, stability and instability depending on the operating point [1-5]. Therefore, it is one of the highly difficult processes for control.

If a conventional controller with fixed parameters is operated on such a process over the whole operating points, it may not only become unstable but also does not provide good performance in some cases. Therefore, in order to design a controller with more precise and stable control performance, there have been a lot of efforts applying intelligent techniques such as evolutionary algorithms, neural networks, and fuzzy [6-12].

Banu and Uma [6] proposed a gain scheduling method in the process of controlling the concentration of the CSTR, where high, medium and low density area are separated for the local model and proposed a method for tuning a PID controller with a GA. Nekoui et al. [10] proposed a method for optimizing the tuning parameters of a PID controller to control the CSTR concentration using a PSO (particle swarm optimization) algorithm. Saoud et al. [12] proposed an embedded system based on a microcontroller with a

neural network, where the neural network is trained by back-propagation algorithm. Chen and Peng [11] proposed a method for learning control of the non-linear adaptive controller (bounded nonlinear controller) with a limit value in order to control the water outlet temperature of a CSTR, where the learning algorithm for a process of change is obtained based on Lyapunov stability theory.

Recently, there has been a trend towards using nonlinear PID (NPID) control schemes for processes which have highly nonlinear and time-varying characteristics during operation [15-19]. To improve the control performance, Aydogdu and Korkmaz [15,16] proposed a dynamic NPID controller that changes parameters over time according to the error response. Li et al. [17] presented an NPID controller made of the combination of linear proportional and linear derivative terms was used with an integral term whose gain was tuned by a nonlinear Gaussian function. Chen et al. [18] proposed nonlinear PID control which combines a series of nonlinear functions for an electro-hydraulic servo system where three gains are adjusted according to the error. So et al. [19] also proposed a practical NPID controller whose three gains are adjusted by the error and error rate. The parameters of the three gains are tuned by a real-coded genetic algorithm.

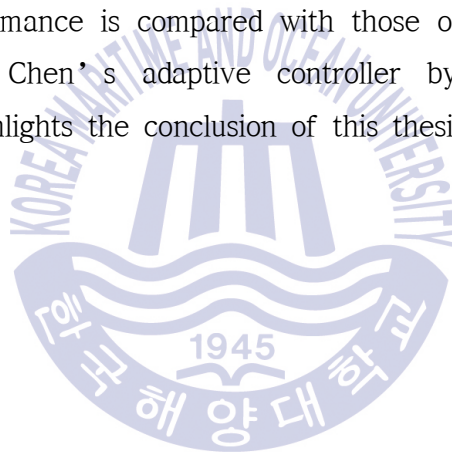
Each method presents its own satisfactory performance in different control scheme but it may leave room for further improvement.

1.2. Method and Organization

This thesis presents a scheme of designing a nonlinear PID controller incorporating with a real-coded genetic algorithm (RCGA) for the temperature control of a CSTR process. The gains of the proposed NPID controller are expressed by easily implementable nonlinear functions based on the error and/or the error rate and the parameters of the NPID controller are tuned using the RCGA by minimizing the integral of time-weighted absolute error

(ITAE) as a objective function. A set of simulation works for reference tracking and disturbance rejecting performances and robustness to parameter changes are carried out to compare with two nonlinear controllers and show the feasibility of the proposed method.

Chapter 2 gives a brief overview of a continuous stirred tank reactor as the controlled process in this thesis, Chapter 3 describes about the linear PID controller which lays foundation for nonlinear PID controllers and two nonlinear controllers for comparison. Chapter 4 proposes an NPID controller which improves the nonlinear gain function proposed by Korkmaz et al. and discusses how to optimize parameters of the NPID controller. Chapter 5 applies the proposed NPID controller to control the temperature of the CSTR process and its performance is compared with those of both the Korkmaz's NPID controller and Chen's adaptive controller by computer simulation. Finally, Chapter 6 highlights the conclusion of this thesis.



Chapter 2. Continuous Stirred Tank Reactor

CSTR (Continuous Stirred Tank Reactor) is a key device, which has been widely used for pyrolytic reaction and catalyst-using polymer synthesis in petrochemical process as it has advantage in removing severe heat of reaction and facilitating rapid heating and cooling. This chapter gives a brief overview of CSTR which is used as a controlled process in this thesis.

2.1. Process Description

As chemical reaction which occurs in a CSTR is exothermic or endothermic, it has to be cooled or heated by external media to maintain constant temperature in the reactor. Figure 2.1 shows the schematic diagram of a CSTR process, where exothermic reaction is assumed. In the Figure, C_f , T_f , F_f and C , T , F denote concentration[mol/m³], temperature[K] and flow[m³/sec] at the inlet and outlet of fluid, respectively and T_{cf} , F_{cf} and T_c , F_c denote the temperature and flow at the inlet and outlet of cooling water, respectively.

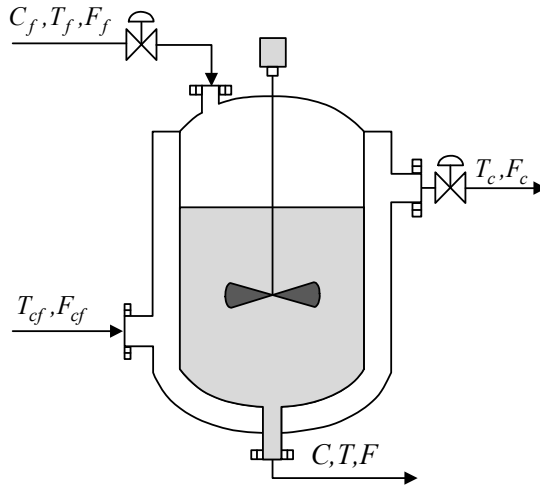


Fig. 2.1 Nonisothermal CSTR process

It is assumed to simplify the problem in this thesis that irreversible reaction ($A \rightarrow B$) is exothermic, reaction is considered 1st-order to the reactant, fluid in the reactor is well stirred, input and output flow are identical and parameters are constant and independent of temperature, the following dimensionless form of equation is obtained by applying the law of conservation of matter and energy to CSTR [1,2,5,11]:

$$\dot{x}_1 = -x_1 + D_a(1-x_1)\exp\left(\frac{x_2}{1+x_2/\gamma}\right) + d_1 \quad (2.1a)$$

$$\dot{x}_2 = -(1+\beta)x_2 + HD_a(1-x_1)\exp\left(\frac{x_2}{1+x_2/\gamma}\right) + \beta u + d_2 \quad (2.1b)$$

$$y = x_2 \quad (2.1c)$$

where, x_1 and x_2 are state variables which indicate concentration C and temperature T , respectively and y and u indicate the outlet temperature of fluid and the temperature of cooling water as the output and input,

respectively. d_1 and d_2 denote disturbances. At this time, x_1 , x_2 , u and t are nondimensionalized by Equation (2.2):

$$x_1 = \frac{C_f - C}{C_f} \quad (2.2a)$$

$$x_2 = \frac{T - T_f}{T_f} \gamma \quad (2.2b)$$

$$u = \frac{T_c - T_f}{T_f} \gamma \quad (2.2c)$$

$$t = t' \frac{F_f}{V} \quad (2.2d)$$

where D_a denotes Damökhler number, H heat of reaction, β heat transfer coefficient, V volume of CSTR[m³], $\gamma = E/RT_f$, E activation energy[cal/mol] and R gas constant[cal/mol-K].

As the CSTR process discussed in this thesis controls the outlet temperature (T_c) of the cooling jacket as a control input, the flow-changing valve operation has physical limit. Therefore, it is assumed that there is a saturator represented by the following nonlinear equation between the controller and CSTR process

$$u_{sat} = \begin{cases} u_{min} , & u < u_{min} \\ u , & u_{min} \leq u \leq u_{max} \\ u_{max} , & u > u_{max} \end{cases} \quad (2.3)$$

where u_{min} and u_{max} indicate the minimum and maximum values of the saturator,

respectively and u_{sat} indicates the output of the saturator or input of the process. Therefore, the process is represented by Figure 2.2 through combining the saturator and CSTR process.

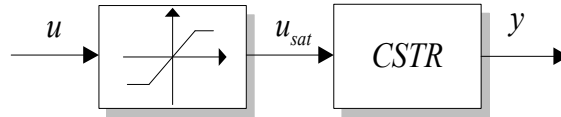


Fig. 2.2 Block diagram of the CSTR process with a saturator

2.2. Analysis of the Process

If the open-loop system represented by Equation (2.1) has values of $D_a = 0.072$, $\gamma = 20$, $H = 8$ and $\beta = 0.3$, it becomes a complex process which has three equilibrium points of $\mathbf{x}_{eA} = [0.144, 0.886]^T$, $\mathbf{x}_{eB} = [0.447, 2.752]^T$ and $\mathbf{x}_{eC} = [0.765, 4.705]^T$. \mathbf{x}_{eA} and \mathbf{x}_{eC} are stable equilibrium points but \mathbf{x}_{eB} is an unstable equilibrium point. Figure 2.3 shows three equilibrium points on phase diagram.

Figure 2.4 shows the open-loop response y of the CSTR to step input changes of u where it can be shown that the response speed and steady-state gain obviously change according to the magnitude of u . Due to this nonlinearity, it can be guessed that the conventional PID controller with fixed gain may have a difficulty in controlling the CSTR at the overall operating points.

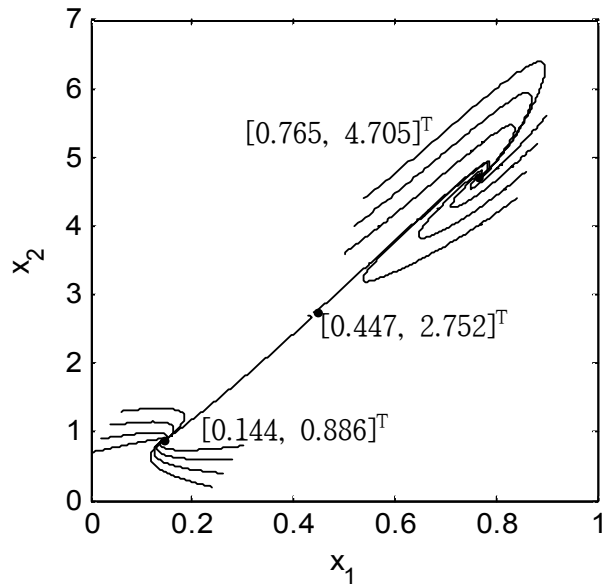


Fig. 2.3 Phase-portrait for three equilibrium points

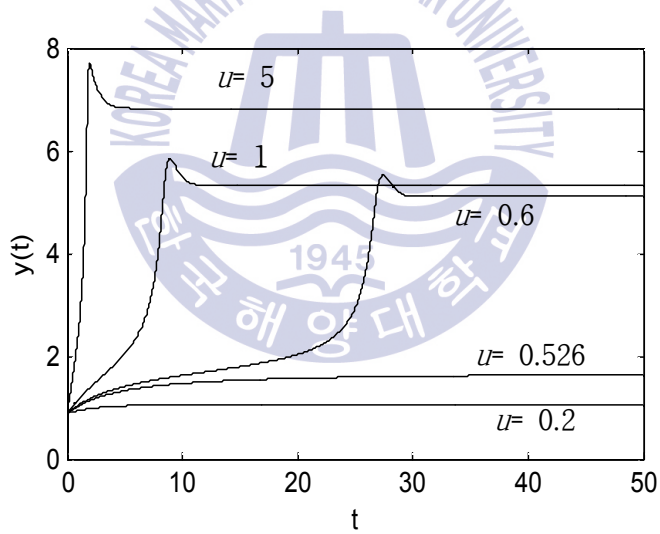


Fig. 2.4 Step responses of the CSTR

Chapter 3. Existing Controllers

This chapter gives a brief description about the linear PID controller which lays foundation for nonlinear PID controllers and two nonlinear controllers for comparison which will be discussed in Chapter 5.

3.1. Linear PID Controller

3.1.1. Structure of the linear PID controller

The transfer function of the standard linear PID (LPID) controller is given by the following equation:

$$C(s) = K_p + \frac{K_i}{s} + K_d s \quad (3.1)$$

where K_p is the proportional gain, K_i the integral gain and K_d the derivative gain.

The LPID controller involves three separate control actions, that is, proportional action u_p , integral action u_i and derivative action u_d . It can be expressed as the block diagram shown in Figure 3.1.

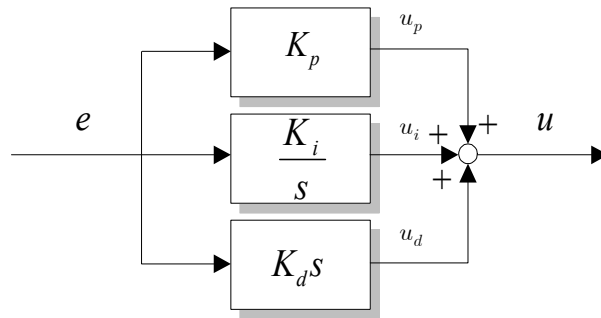


Fig. 3.1 Structure of the standard LPID controller

The LPID controller receives error signal and makes control input so that the output of the process follows the set-point with user-defined specific requirements. Generally, three gains of the LPID controller are fixed for use during operation, and if gain scheduling technique is used, it is possible to switch among gains tuned according to operation points.

3.1.2. Role of the LPID control action

As shown in the previous Figure, LPID consists of parallel combination of three control actions. Among them, proportional action u_p , which is performed in proportion to e , speeds up the process response and reduces settling time, but if too big, it will make the closed-loop system unstable. Integral action u_i is output in proportion to the integration value of e from the initial time to the present time, removes error in steady-state, but if too big, causes ziggling and enlarges overshoot. Derivative action u_d reduces vibration and overshoot to improve transient response. Figure 3.2 shows the example of three control actions of the LPID controller in a closed-loop control system in a graphical form.

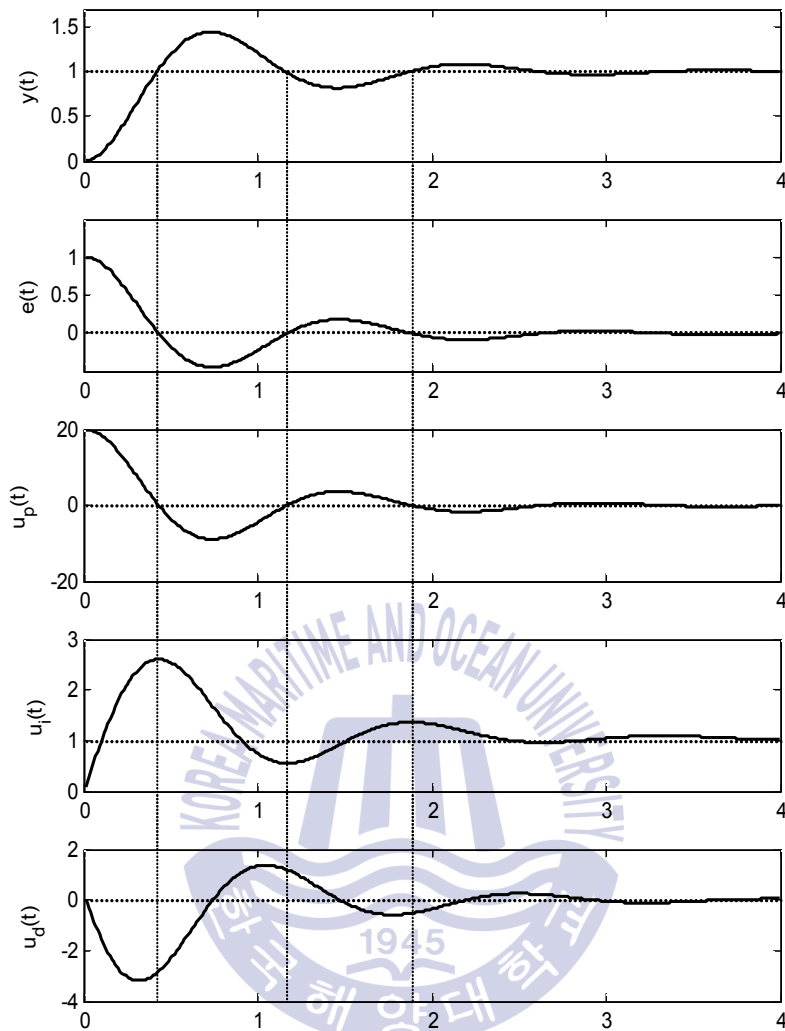


Fig. 3.2 Example of three control actions of the LPID controller

3.1.3. Ziegler-Nichols (Z-N) tuning rules

We simply discuss the well-known existing tuning rules for the LPID controller. In 1942, Ziegler and Nichols proposed the two methods to determine the parameters of a PID controller from the form of transient response indicated by a process. The Z-N tuning methods [13] have advantage of requiring no knowledge of the underlying process and are widely used in PID controller design. Those tuning methods are roughly classified into the

open-loop method and closed-loop method. The former uses an open-loop response curve obtained offlinely and the latter does only the P control term installed in the process.

① Open-loop method

This method uses the step response curve. First, a step input is applied to the given process to obtain s-curve. Steady-state gain K , time constant T and time delay L are obtained while viewing the output state of the process, and based on these, the parameters of PID controller are tuned. This method can only be applied to a stable system where integrators are not included in the process and main pole is not complex root.

Figure 3.3 shows obtaining K , T and L from the response curve when unit step input is given to the open-loop control system and Table 3.1 shows how to obtain the controller parameters by using these values.

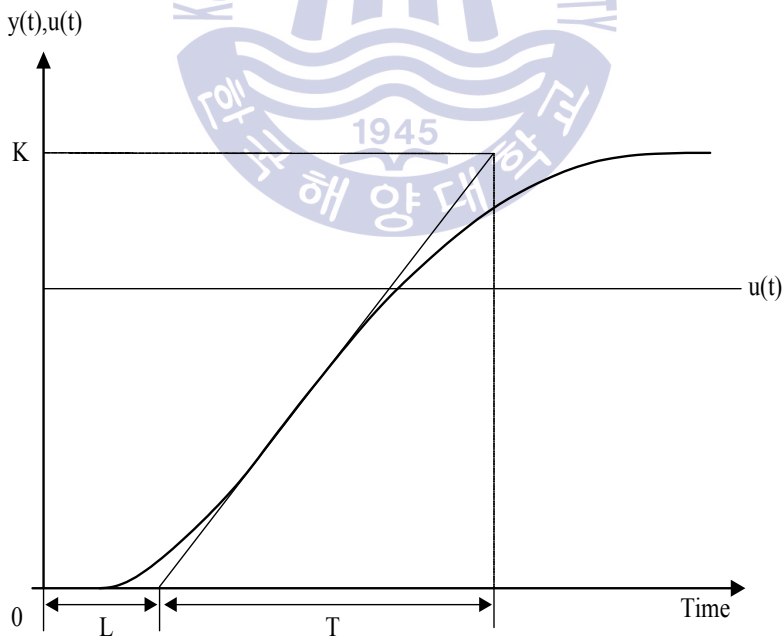


Fig. 3.3 Step response of a process

Table 3.1 PID tuning rules by the open-loop method

Parameter Controller	K_p	T_i	T_d
P	$\frac{\tau}{KL}$	-	-
PI	$0.9 \frac{T}{KL}$	$3.3L$	-
PID	$1.2 \frac{T}{KL}$	$2.0L$	$0.5L$

The open-loop method is a simple tuning method where unit step input is given to the system and parameters of PID controller are obtained from characterization factors of the curve. However, as mentioned previously, this method can only be applied to a stable process which can be approximated to FOPTD (First-Order Plus Time Delay), it has disadvantage of very limited scope of application. The transfer function $G_p(s)$ of a FOPTD system is as follows:

$$G_p(s) = \frac{K}{1 + Ts} e^{-Ls} \quad (3.2)$$

② Closed-loop method

The closed-loop method is a method which can be used even when the process has a pole at origin and is unstable. Unlike the open-loop method, this method first constructs a closed-loop system with only a proportional gain as shown in Figure 3.4.

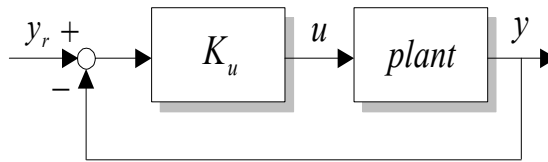


Fig. 3.4 Closed-loop control system with a proportional gain

Then, the proportional gain K_p is increased until it reaches to the ultimate gain K_u , at which the output of the control loop oscillates with a constant amplitude.

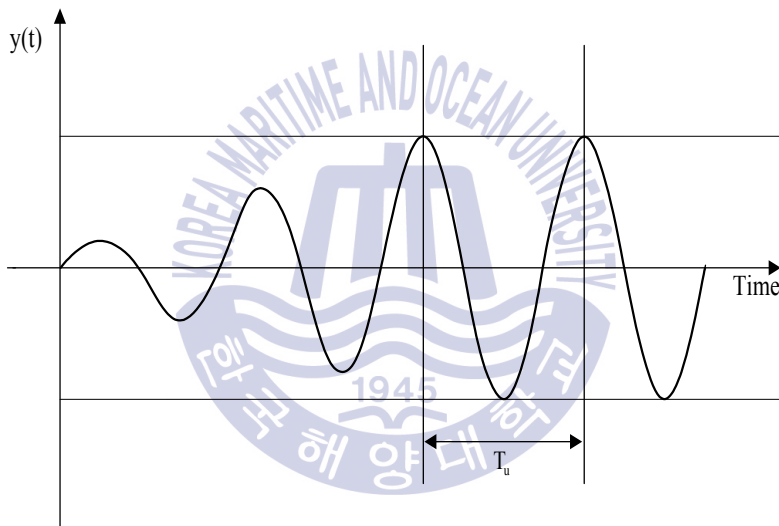


Fig. 3.5 Response curve and ultimate period

After the ultimate period T_u is obtained from the response depicted in Figure 3.5, the PID controller parameters are tuned by applying the rules in Table 3.2.

Table 3.2 Tuning rules by the closed-loop method

Parameter Controller	K_p	T_i	T_d
P	$\frac{1}{2}K_u$	-	-
PI	$\frac{1}{2.2}K_u$	$\frac{1}{1.2}T_u$	-
PID	$\frac{1}{1.7}K_u$	$\frac{1}{2}T_u$	$\frac{1}{8}T_u$

The closed-loop method requires much time as it generates the ultimate cycle by trial and error of many experimental values and has a difficulty in maintaining vibration within the stability limit of gain in actual processes. If the controller is replaced by a relay controller, there will be a stable oscillation in the output response. The amplitude of this oscillation together with the magnitude of the relay can be used to determine the ultimate gain K_u as

$$K_u = \frac{4d}{\pi a} \quad (3.3)$$

where d denotes the magnitude of the relay and a the amplitude of the response.

3.2. Nonlinear PID Controller

As the previously mentioned LPID controller is used with fixed gains in most cases, it may show unsatisfactory performance if parameters of the process change due to changes of operating point. To solve these problems, nonlinear PID (NPID) controllers take the method of changing three gains nonlinearly for control. Although several methods have been proposed in recent literatures, in

this thesis, we briefly review the NPID controller proposed by Korkmaz et al. [15] (simply referred to as Korkmaz' s NPID controller) and nonlinear adaptive controller proposed by Chen et al. [11] (simply referred to as Chen' s adaptive controller) as comparison purpose.

3.2.1. Korkmaz' s NPID controller

The method proposed by Korkmaz et al. [15] takes the method of changing three gains of the existing LPID controller nonlinearly and the controller is given by Equation (3.4)

$$C(s) = K_p(e) + \frac{K_i(e)}{s} + K_d(e)s \quad (3.4)$$

where $K_p(e)$, $K_i(e)$ and $K_d(e)$ are nonlinear functions based on error e and Gaussian error function, and play the same roles as proportional, integral and derivative gains of the LPID controller.

$$K_p(e) = a_1 + a_2 \operatorname{erf}(e) \quad (3.5a)$$

$$K_i(e) = b[1 - \operatorname{erf}(e)] \quad (3.5b)$$

$$K_d(e) = c[1 + \operatorname{erf}(e)] \quad (3.5c)$$

where parameters a_1 , a_2 , b , c are all positive constants and properly tuned by the user. $\operatorname{erf}(e)$ is the Gaussian error function defined as

$$\operatorname{erf}(e) = \frac{2}{\sqrt{\pi}} \int_0^e \exp(-t^2) dt \quad (3.6)$$

and has the shape as shown in Figure 3.6.

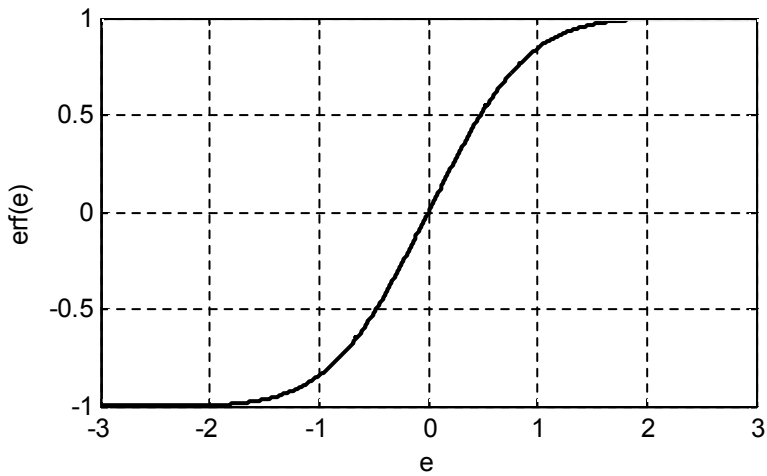


Fig. 3.6 Gaussian error function

Figure 3.7 shows the change of nonlinear gain values according to the change of error. From the Figure, it can be shown that proportional gain and derivative gain increase when the absolute value of error increases and integral gain increases to reduce steady-state deviation when the absolute value of error decreases.

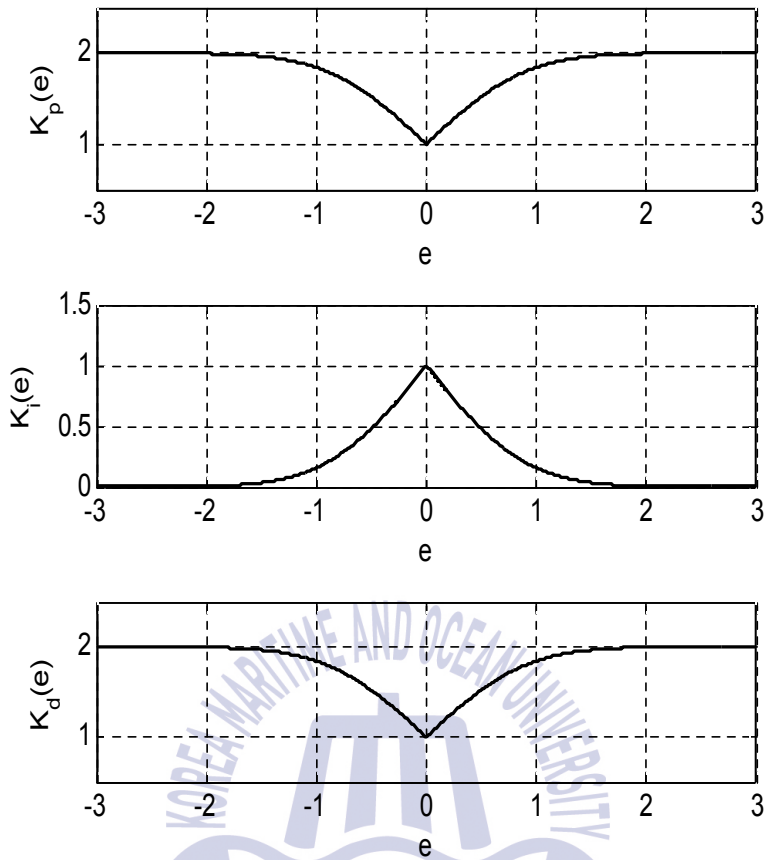


Fig. 3.7 Nonlinear gain functions proposed by Korkmaz et al.

Korkmaz et al. used the absolute value of error $|e|$ instead of error e to make PID gain a positive constant, and due to this, only the positive region of $f(e)$ function is used. Therefore, minimum and maximum values of proportional gain $K_p(e)$ are a_1 and $a_1 + a_2$, respectively. The range of integral gain $K_i(e)$ is 0 and b . Derivative gain $K_d(e)$ varies in the range of c and $2c$.

3.2.2. Chen' s adaptive controller

Recently, Chen and Peng[11] proposed a controller for the adaptive control of a system with the saturator size of $u_{\min} \leq u(t) \leq u_{\max}$ as shown in Figure 3.8.

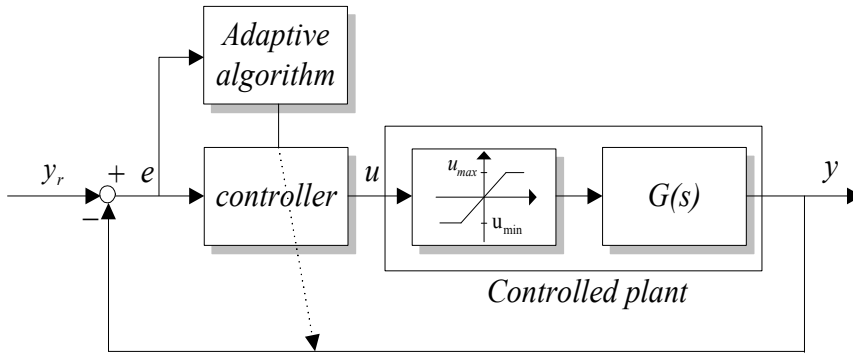


Fig. 3.8 Adaptive control system proposed by Chen and Peng

The control input is given as the following equation:

$$u(t) = \frac{1}{2}[(1 + \tilde{u}(t))u_{\max} + (1 - \tilde{u}(t))u_{\min}] \quad (3.7)$$

where $\tilde{u}(t)$ is a hyperbolic tangent function given as follows:

$$\tilde{u}(t) = \frac{1 - \exp[-m(e(t) - \theta(t))]}{1 + \exp[-m(e(t) - \theta(t))]} \quad (3.8)$$

where $e(t)$ denotes error between the set-point and output. m and $\theta(t)$ denote slope and bias, respectively. As $\tilde{u}(t)$ has a value between -1 and 1, $u(t)$ in Equation (3.7) is maintained within the limit value of the saturator.

As shown in Equation (3.8), as $\tilde{u}(t)$ has two adjusting parameters, and particularly, the size and sign of slope m are highly sensitive to the characteristics of the controller, Chen and Peng proposed an algorithm to adaptively control bias $\theta(t)$ with fixed m alone according to control problems. Figure 3.9 shows the slope of $\tilde{u}(t)$ when $\theta(t)$ is fixed to 0 and m is changed.

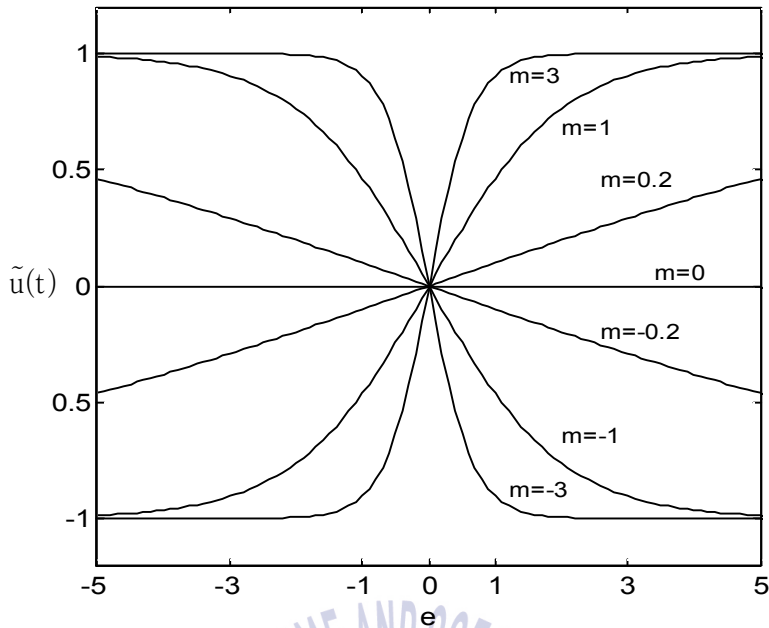


Fig. 3.9 Significance of $\tilde{u}(t)$ to the changes of m ($\theta = 0$)

The tuning algorithm of $\theta(t)$ is given by

$$\dot{\theta}(t) = -\eta m e(t) (1 - \tilde{u}(t)) (1 + \tilde{u}(t)) \text{sign}\left(\frac{\partial y}{\partial u}\right) \quad (3.9)$$

where $\eta (> 0)$ is learning rate and $\text{sign}\left(\frac{\partial y}{\partial u}\right)$ has a value of ± 1 which is determined by the response direction of the system. $\text{sign}\left(\frac{\partial y}{\partial u}\right)$ is obtained by step response test or physical characteristics of the process. In this way, the algorithm continuously adjusts parameters of the controller with the error between set-point and actual output.

As Chen and Peng used $\eta = 0.2$ and $m = 5$ when they applied to the temperature control problem of a CSTR and the CSTR process has positive gain by its characteristics, $\text{sign}\left(\frac{\partial y}{\partial u}\right)$ becomes 1.

Chapter 4. Proposed NPID Controller

This chapter presents an NPID controller which improves the nonlinear gain function proposed by Korkmaz et al. and discusses how to optimize parameters of the NPID controller.

4.1. Structure of the Proposed NPID Controller

In this thesis, we use an NPID controller represented by Equation (4.1) for temperature control of the CSTR and improve set-point tracking performance. The transfer function $C(s) = U(s)/E(s)$ of the NPID controller consists of parallel combination of proportional, integral and derivative actions which have the same meanings as those of three actions in the LPID controller:

$$C(s) = K_p(e) + \frac{K_i(e)}{s} + \frac{K_d(e, \dot{e})s}{1 + T_f(e, \dot{e})s} \quad (4.1)$$

where $K_p(e)$, $K_i(e)$, $K_d(e, \dot{e})$ and $T_f(e, \dot{e})$ are nonlinear functions of error e and the rate of change of error \dot{e} and time-varying gains. $T_f(e, \dot{e}) = T_d(e, \dot{e})/N$ is the filter time constant. Maximum derivative gain N is an empirically determined constant between 8 and 20. As many literatures use $N=10$, we also adopt this value here.

The transfer function in Equation (4.1) can be expressed in a block diagram as shown in Figure 4.1.

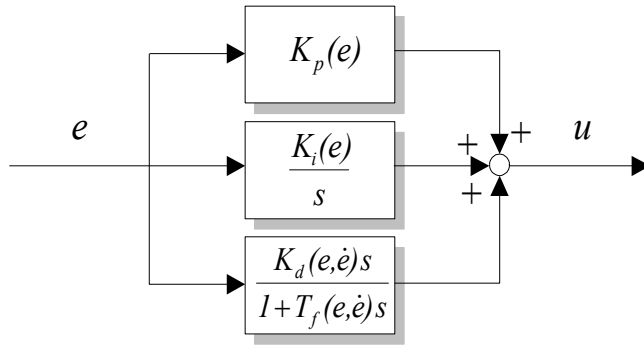


Fig. 4.1 Structure of the proposed NPID controller

4.2. Gains of the Proposed NPID Controller

4.2.1. Nonlinear proportional gain

Since control action u_p increases in proportion to proportional gain or error, and to speed up response, proportional gain needs to be properly enlarged when error is large. However, if a large proportional gain is maintained even for a small error when the response reaches around set-point, excessive control may cause overshoot and vibration.

By considering this fact, the proportional gain $K_p(e)$ of the NPID controller is properly adjusted according to the magnitude of e and defined by

$$K_p(e) = a_1 + a_2 f(e) \quad (4.2)$$

where a_1, a_2 are positive constants determined by the user. $f(e)$ is described by an exponential function as:

$$f(e) = 1 - \exp(-4e^2) \quad (4.3)$$

where $f(e)$ is a symmetrical nonlinear function centered upon $e=0$. It goes to zero as e goes to 0. As e increases, the value increases, converging to 1. Therefore, $K_p(e)$ in Equation (4.2) has the minimum value of a_1 when $e=0$ and the maximum value of a_1+a_2 when $e \rightarrow \infty$.

Figure 4.2 shows the shape of the proportional gain function $K_p(e)$ to changes of e with $a_1=2$ and $a_2=1$. For comparison, $K_p(e)$ in Equation (3.5a) is also drawn.

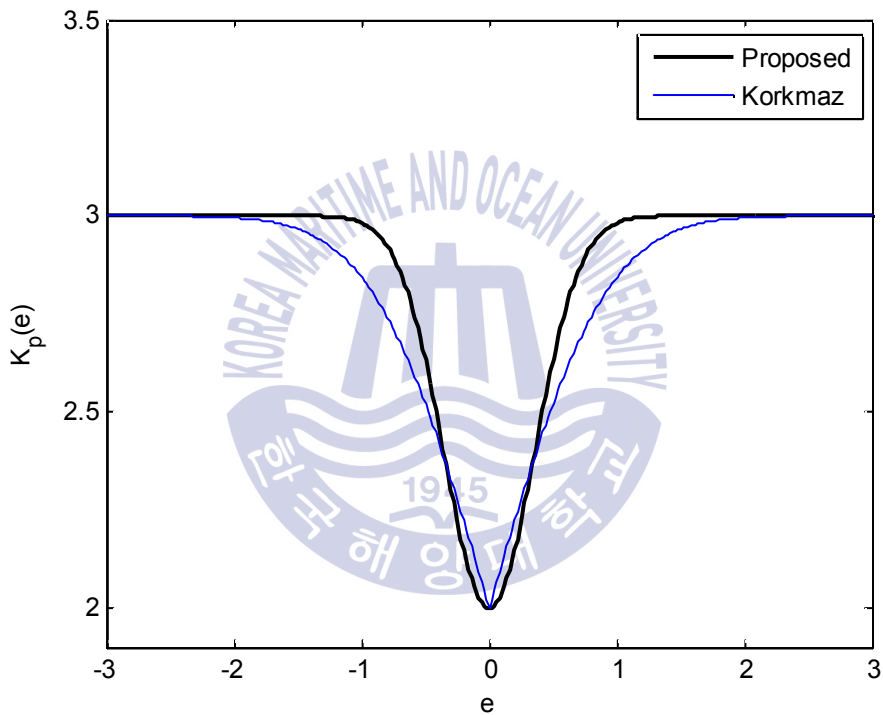


Fig. 4.2 $K_p(e)$ shapes to changes of e ($a_1=2$, $a_2=1$)

From the Figure, it can be seen that the proposed nonlinear function $K_p(e)$ has steeper slope around $e=0$ than that of Korkmaz responding more sensitively to small change.

4.2.2. Nonlinear integral gain

Integral action u_i increases as cumulative error value or integral gain increases. Equation (4.4) is used to ensure that integral gain is decreased to prepare for the occurrence of overshoot when the absolute value of error e is large and the gain is enlarged to reduce steady-state error when the absolute value of error e is small. The nonlinear integral gain is expressed by

$$K_i(e) = b[1 - f(e)] \quad (4.4)$$

where b is a positive constant and Equation (4.3) is used for function $f(e)$.

Figure 4.3 shows $K_i(e)$ to changes of e with $b=1$. As shown in the Figure, it has the maximum value when $e=0$ and decreases as the absolute value of e increases.

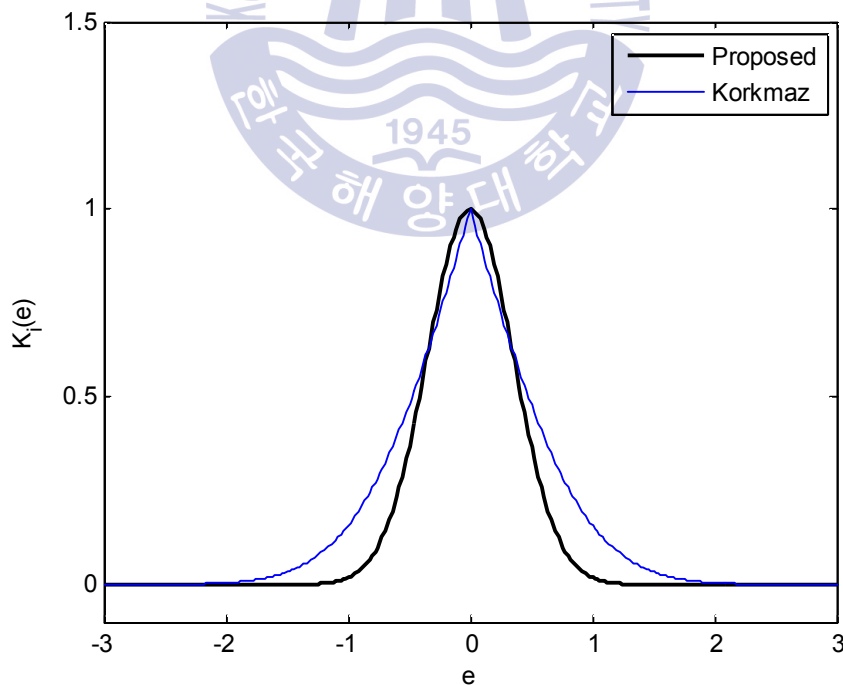


Fig. 4.3 $K_i(e)$ shapes to changes of e ($b=1$)

4.2.3. Nonlinear derivative gain

Derivative action u_d increases in proportion to the rate of change of error and derivative gain, and if u_p and u_i increase, damping is performed by predicting that the output will also increase. If damping is performed more than required level over the entire control cycle, response may be slowed down. If damping is only performed for a certain cycle, u_p and u_i can be utilized more drastically and overshoot can also be reduced. Therefore, a time-varying function described by Equation (4.5) is used to change the size of derivative gain to ensure that large damping is performed in the area where $e\dot{e} > 0$. Therefore, $K_d(e, \dot{e})$ is given by

$$K_d(e, \dot{e}) = \begin{cases} c_1 + c_2 f(e), & e\dot{e} > 0 \\ c_1, & \text{elsewhere} \end{cases} \quad (4.5)$$

where c_1, c_2 are positive constants and nonlinear gain $K_d(e, \dot{e})$ is $c_1 + c_2 f(e)$ when multiplication of error e and the rate of change of error \dot{e} is larger than 0. At the time, as $f(e)$ has a value in the range of 0 and 1, $K_d(e, \dot{e})$ becomes c_1 when $e = 0$ and has the value of $c_1 + c_2$ when $e \rightarrow \infty$. For other cases, it becomes c_1 .

Figure 4.4 shows drawing of $K_d(e, \dot{e})$ while changing error e and the rate of change of error \dot{e} .

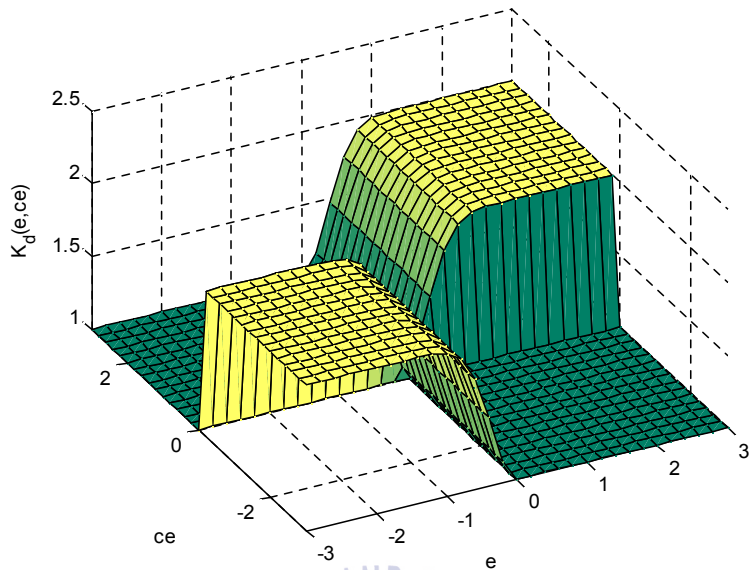


Fig. 4.4 $K_d(e, \dot{e})$ shapes to changes of e ($c_1 = c_2 = 1$)

4.3. Tuning of the NPID Controller Parameters

As previously mentioned, the three nonlinear gains of the proposed NPID controller have total five parameters and these parameters should be properly adjusted to ensure that the entire control process including the saturator can maintain the desired set-point tracking performance.

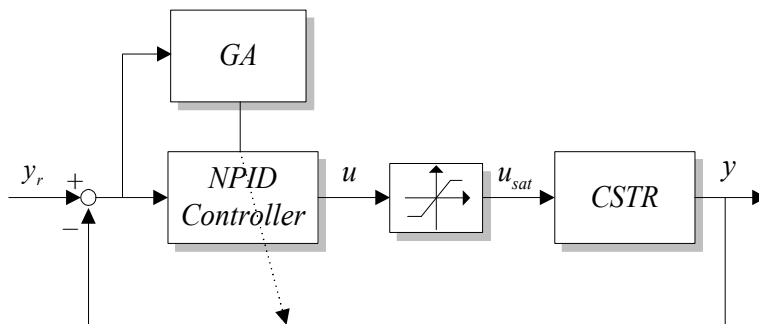


Fig. 4.5 Tuning of the proposed NPID controller with a saturator

This leads to a nonlinear multi-variable optimization problem and it will be solved by applying a Genetic Algorithm (GA). The Integral of Time-weighted Absolute Error (ITAE) is used as an evaluation function which measures the closed-loop system performance.

$$J(\phi) = \int_0^{t_f} t|e(t)| dt \quad (4.6)$$

where $\phi = [a_1, a_2, b, c_1, c_2]^T \in \mathbb{R}^5$ is a vector which consists of parameters of NPID controller gains, $e(t)$ is error between the set-point $y_r(t)$ and output $y(t)$, and integral time t_f is a value sufficiently large enough to ignore integral afterwards.

The most basic decision in applying a GA to optimization problems under consideration is whether to use binary or real coding to represent the parameters to be optimized. If the search space of an optimization problem is continuous and wide, a Real-Coded GA (RCGA) is possibly more acceptable. Therefore, in this thesis real number encoding is adopted rather than traditional binary encoding. Each chromosome comprises of five parameters, a_1, a_2, b, c_1 and c_2 with different value bounds.

Also, one of crucial steps is to construct the population. Some previous works recommend 20 to 100 chromosomes in a population. The more the chromosomes number, the better the chance to find the optimal results. However, as long as the execution time is considered, we keep 50 chromosomes in each generation.

Chapter 5. Simulation and Review

In this chapter, the NPID controller designed in the previous chapter is applied to control the temperature of a CSTR process and its performance is compared with those of both the Korkmaz' s NPID controller and Chen' s adaptive controller through a set of computer simulation works.

5.1. Parameters for Simulation and Controller Tuning

5.1.1. Parameters for simulation

For the data of the CSTR used as process in simulation, $D_a= 0.072$, $\gamma= 20$, $H= 8$ and $\beta= 0.3$ were used. The upper and lower limits of the saturator were ± 5 and sampling interval was 0.01.

5.1.2. NPID controller tuning

Both the proposed NPID controller and Korkmaz' s NPID controller are tuned for good tracking performance and the same set-point in Figure 5.1 was used for fairness in comparison. At $t= 0$, when the process stays at equilibrium point x_{eA} , the set-point is changed to $y_r= 2.752$ to move to equilibrium point x_{eB} . And at $t= 10$, it is changed to $y_r= 4.705$ to move to equilibrium point x_{eC} for tuning.

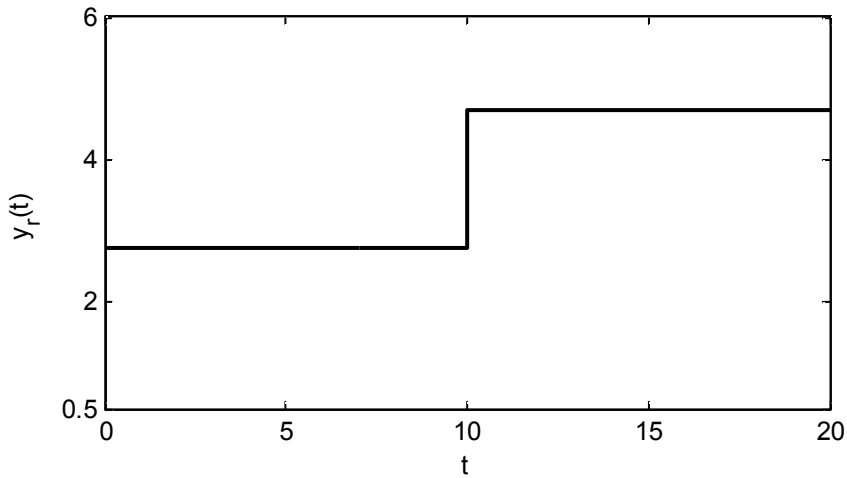


Fig. 5.1 Changing the set-point for parameter tuning

For the control parameters of the RCGA used for tuning, population size $P_{size} = 40$ and crossover probability $P_c = 0.9$ were used. For the parameters of dynamic mutation, $P_m = 0.05$ and $b = 5$ were used [11] and the gain parameters of the two NPID controllers were searched from the range $0 < a_1, c_1 \leq 60$, $0 < a_2, c_2 \leq 30$ and $0 < b \leq 100$.

The results of RCGA-based tuning of the NPID controllers are shown in Table 5.1.

Table 5.1 Tuned parameters of the proposed NPID controller and Korkmaz' s NPID controller

Method	Parameters				
	a_1	a_2	b	c_1	c_2
Proposed	59.73	8.48	57.26	8.88	15.51
Korkmaz	35.87	21.70	43.33	2.73	2.73

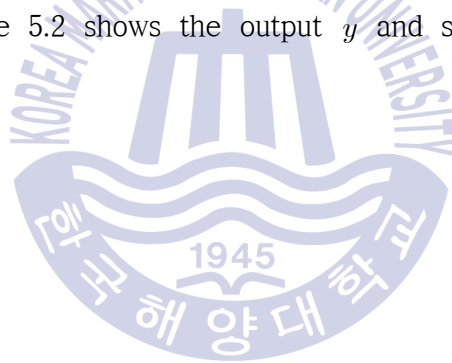
As Chen used $\eta = 0.2$ and $m = 5$ for the algorithm in Equation (3.11) when

applying the adaptive controller to a CSTR process with the saturator and the CSTR process has positive gain by its characteristics, $\text{sign}(\frac{\partial y}{\partial u})$ becomes 1.

5.2. Simulation and Performance Comparison

5.2.1. Set-point tracking performance

First, set-point tracking test was performed by considering the control environment to change temperature at the CSTR cooling water outlet. For the test, the set-point was increased step-wisely to $y_r = 2.75$ when the process stays at a stable equilibrium to move output y to an unstable equilibrium \mathbf{x}_{eB} , and at $t = 10$, it was increased step-wisely to $y_r = 4.705$ to move to a stable equilibrium \mathbf{x}_{eC} . Figure 5.2 shows the output y and saturator output u_{sat} at the same time.



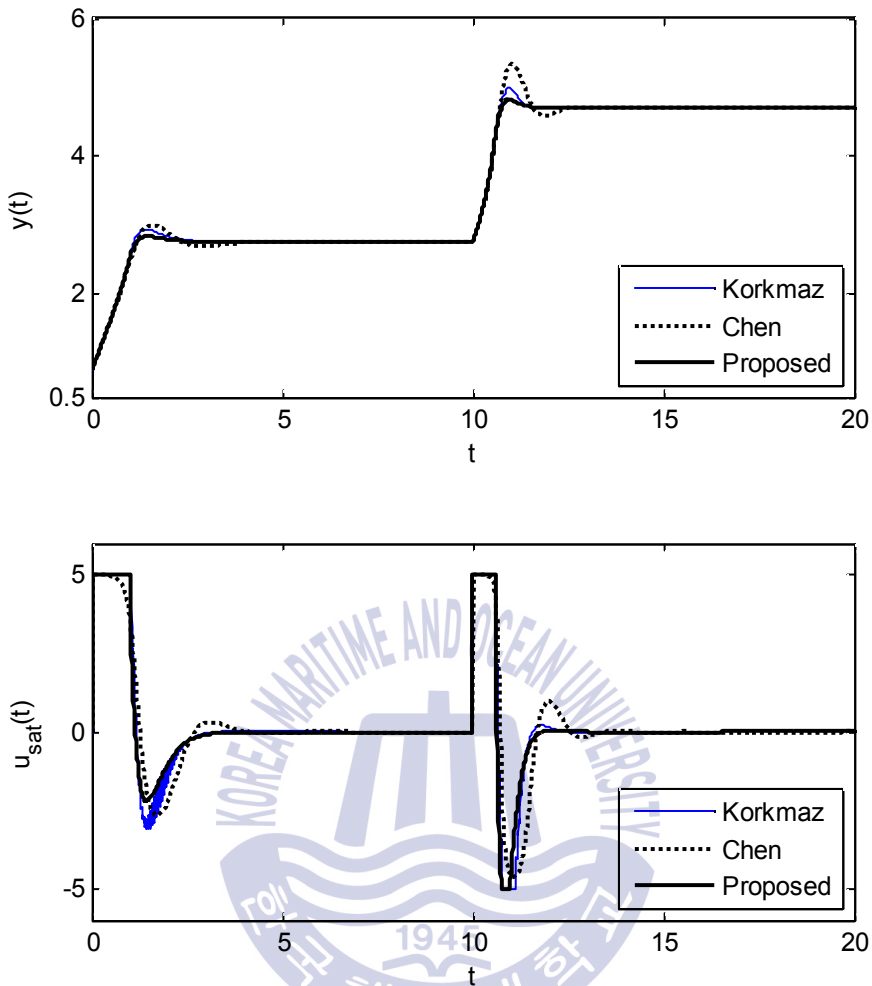


Fig. 5.2 Set-point tracking responses when $y_r(t)$ is step-wisely increased from 0.886 to 4.705

From the Figure, it can be seen that responses of the two NPID controllers and adaptive controller reach the set-point without steady-state error over time, but the proposed method reaches with smaller overshoot and at a faster pace than other methods. Particularly, the reason why overshoot of response is larger when x_{eA} changes to x_{eB} than when x_{eB} changes to x_{eC} is thought to be the intrinsic nonlinearity of the CSTR.

To measure the quantitative performance of three methods, both swiftness

of response and closeness to the set-point were obtained. For swiftness, reaching time(t_r) and peak time(t_p) indexes were used. For closeness, overshoot(M_p), 2% settling time(t_s) and IAE (Integral of Absolute Error) were used. Table 5.2 summarizes simulation results.

Table 5.2 Comparison of set-point tracking performances when y_r is step-wisely increased from 0.886 to 4.705

Method	$y_r = 0.886 \rightarrow 2.75$					$y_r = 2.75 \rightarrow 4.705$				
	t_r	t_p	M_p	t_s	IAE	t_r	t_p	M_p	t_s	IAE
Proposed	0.89	1.50	4.47	2.08	1.19	0.54	0.95	6.04	1.35	0.85
Korkmaz	0.89	1.43	9.96	2.39	1.27	0.52	0.97	14.60	1.40	0.92
Chen	0.93	1.61	13.19	3.39	1.38	0.53	1.03	32.80	2.32	1.22

From the Table, it can be seen that the proposed method has superior performance to the other methods in both swiftness and closeness and particularly the adaptive controller results in the worst control performance.

Due to intrinsic nonlinearity of the CSTR, response characteristics may differ from those when y_r is increased and decreased. To examine this, a response test was performed to decrease y_r with the previously tuned parameters as shown in Figure 5.3. The Figure shows the response while decreasing y_r to 2.75 stepwise when the process stays at equilibrium x_{eC} , and again $t= 10$, decreasing to 0.886 stepwise when it stays at x_{eB} .

It can be found that all responses reach set-point without steady-state error over time, but the Korkmaz' s method shows a severe chattering phenomenon at u_{sat} . The too high proportional gain of the LPID controller with the ideal derivative action might cause such a chattering phenomenon.

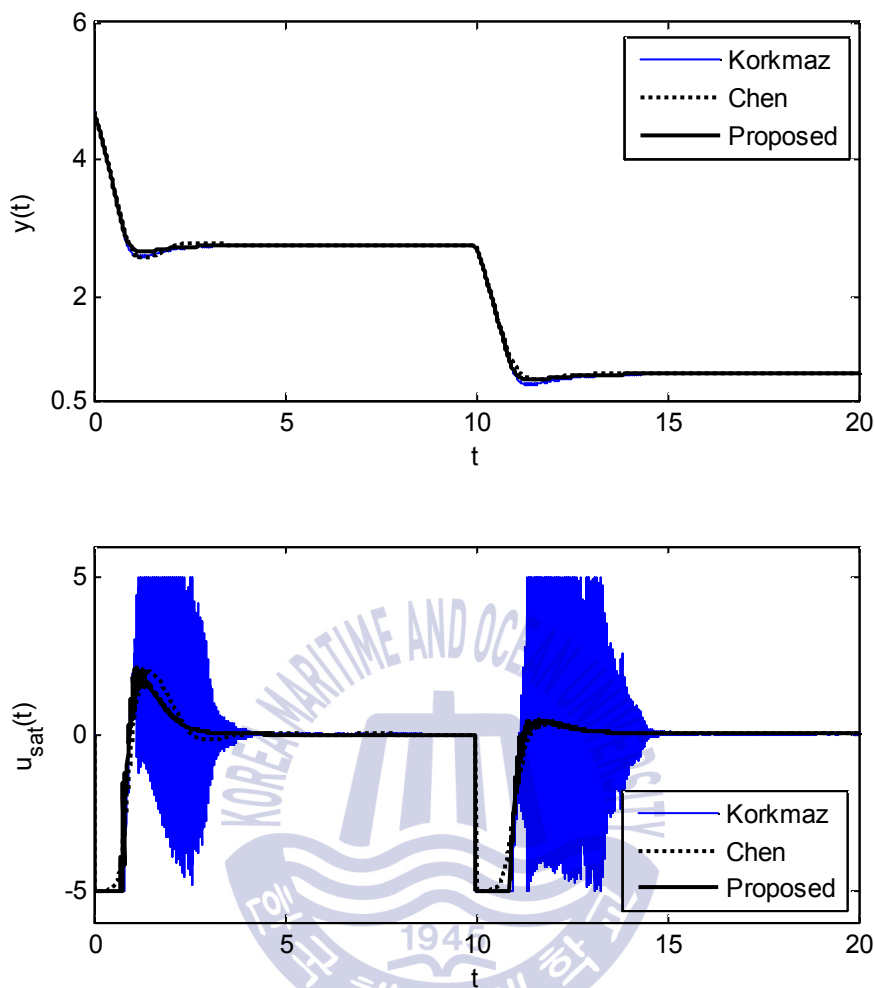


Fig. 5.3 Set-point tracking responses when y_r is step-wisely decreased from 4.705 to 0.886

For this case too, previously used indexes were obtained to measure quantitative performance of three methods and the results are summarized in Table 5.3.

Table 5.3 Comparison of set-point tracking performances when y_r is decreased from 4.705 to 0.886

Method	$y_r = 4.705 \rightarrow 2.75$					$y_r = 2.75 \rightarrow 0.886$				
	t_r	t_p	M_p	t_s	IAE	t_r	t_p	M_p	t_s	IAE
Proposed	0.68	1.32	4.48	2.02	0.99	0.76	1.46	4.77	2.51	1.05
Korkmaz	0.67	1.24	8.38	2.40	1.06	0.76	1.44	8.69	3.06	1.14
Chen	0.70	1.33	9.38	2.98	1.10	0.83	1.60	4.13	2.32	1.05

From the Table, it can be seen that M_p of compared methods have been much reduced than in the previous response test, but the proposed method has overall performance superior to other methods.

5.2.2. Disturbance rejection performance

Next, to examine disturbance rejection performance of the proposed method when unmeasured disturbances are applied to the process due to a variety of factors, two simulation were performed to input disturbance when the process stays at an unstable equilibrium \mathbf{x}_{eB} . For this, the set-point was fixed to $y_r = 2.75$ and two different step-wise disturbances d_1 and d_2 were applied to the right side of Equation (2.1). For first simulation, step-wise disturbance $d_1 = 0.2$ and $d_2 = 0.2$ were applied after $t = 5$ when the process stays at an unstable equilibrium \mathbf{x}_{eB} . For second simulation, $d_1 = 0.2$ and $d_2 = -0.2$ were applied.

Figure 5.4 and 5.5 show each simulation result, that is, output y and saturator output u_{sat} . Figures demonstrate that process disturbances can be effectively attenuated by the proposed method but the other methods require more time to recover from disturbance. Particularly, it can be found that the Chen's adaptive controller has relatively inferior performance to other methods in disturbance rejection performance.

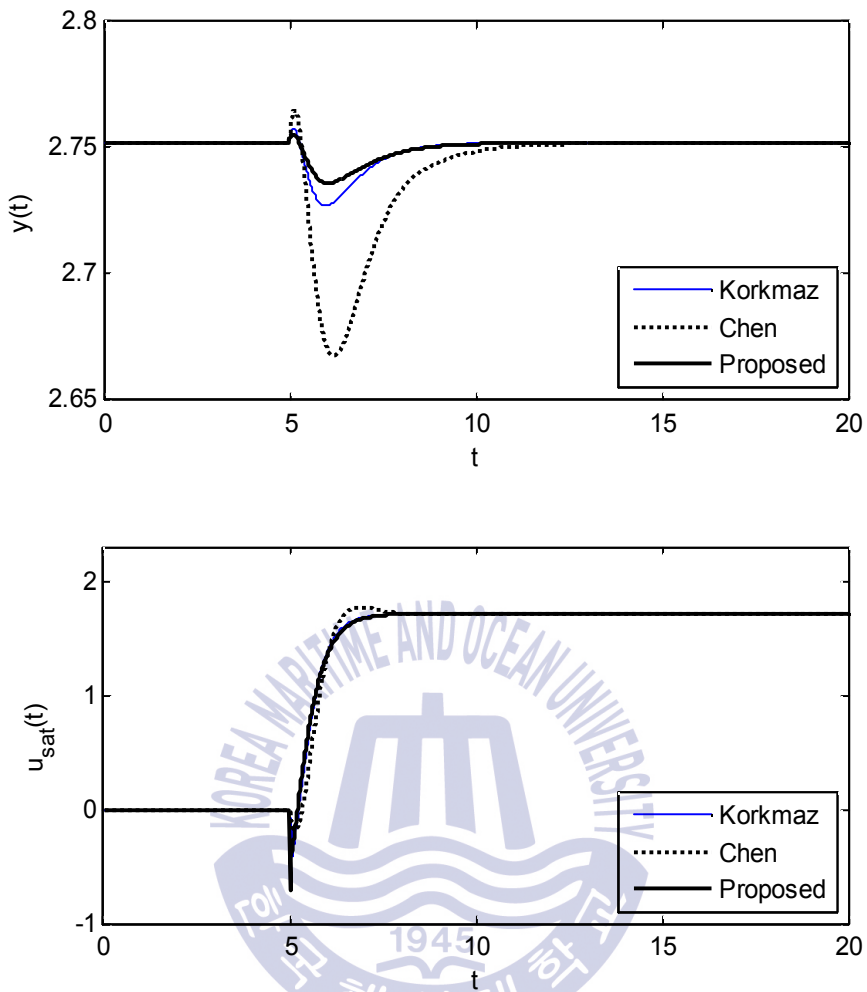


Fig. 5.4 Disturbance rejection responses when d_1 and d_2 are step-wisely changed while $y_r = 2.75$ ($d_1 = d_2 = 0.2$)

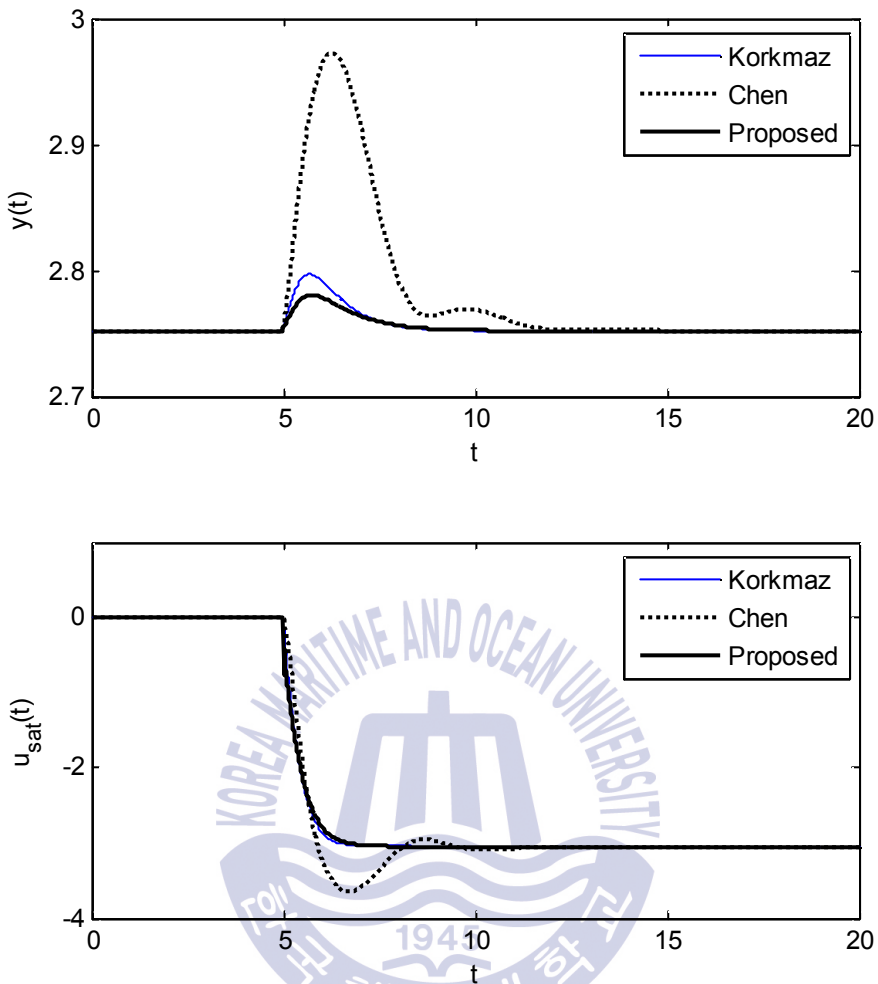


Fig. 5.5 Disturbance rejection responses when d_1 and d_2 are step-wisely changed while $y_r = 2.75$ ($d_1 = -0.2$, $d_2 = 0.2$)

Again, perturbation peak M_{peak} and peak time t_{peak} , recovery time required to remove the effect of disturbance and return to the set-point t_{rcy} , and IAE were obtained in order to measure the performance of three methods quantitatively, where $M_{peak} = |y - y_{max}|$ or $|y - y_{min}|$ and t_{rcy} indicates time required for recovering output y to less than 2% of set-point y_r .

Table 5.4 Comparison of disturbance rejection performances when d_1 and d_2 are step-wisely changed

Method	$d_1 = 0 \rightarrow 0.2, d_2 = 0 \rightarrow 0.2$				$d_1 = 0 \rightarrow -0.2, d_2 = 0 \rightarrow 0.2$			
	t_{peak}	M_{peak}	t_{rcy}	IAE	t_{peak}	M_{peak}	t_{rcy}	IAE
Proposed	1.07	0.02	5.39	0.03	0.77	0.03	4.98	0.05
Korkmaz	1.00	0.02	4.65	0.04	0.71	0.05	4.28	0.07
Chen	1.21	0.08	5.86	0.16	1.29	0.22	6.35	0.48

It can be confirmed from Table 5.4 that the proposed method and Korkmaz's method have good overall performance. Particularly, the Chen's method shows larger M_{peak} as well as longer t_{rcy} .

5.2.3. Robustness to parameter change

As the CSTR is a time-varying process where chemical reaction takes happen and may cause parameter changes during operation, four sets of simulation works were performed to examine the robustness of the proposed method to parameter changes. Figure 5.6 and 5.7 show the results obtained while changing parameter D_a from 0.072 to 0.09 and from 0.072 to 0.05, respectively after $t = 5$ when the control process stays at an unstable equilibrium \mathbf{x}_{eB} . Figure 5.8 shows the response obtained while increasing D_a from 0.072 to 0.09 with raising H simultaneously from 8 to 9 after $t = 5$, and Figure 5.9 shows the response obtained while decreasing D_a from 0.072 to 0.05 with lowering H simultaneously from 8 to 7.

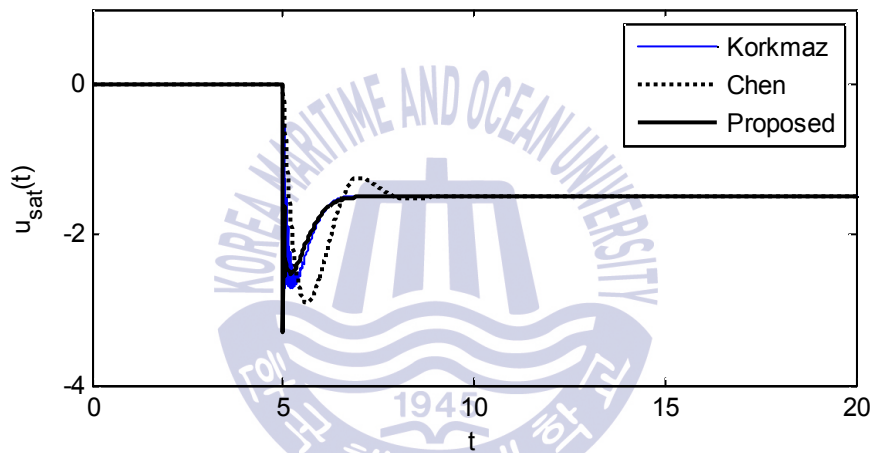
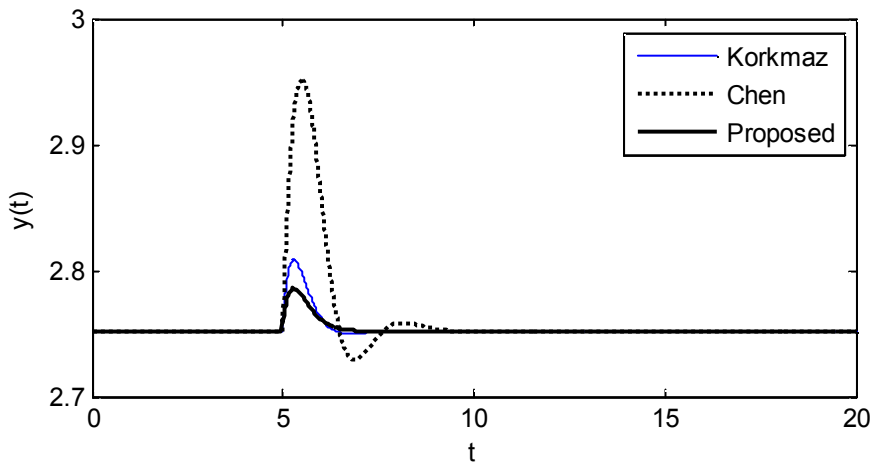


Fig. 5.6 Response comparison to parameter changes ($D_a = 0.072 \rightarrow 0.09$)

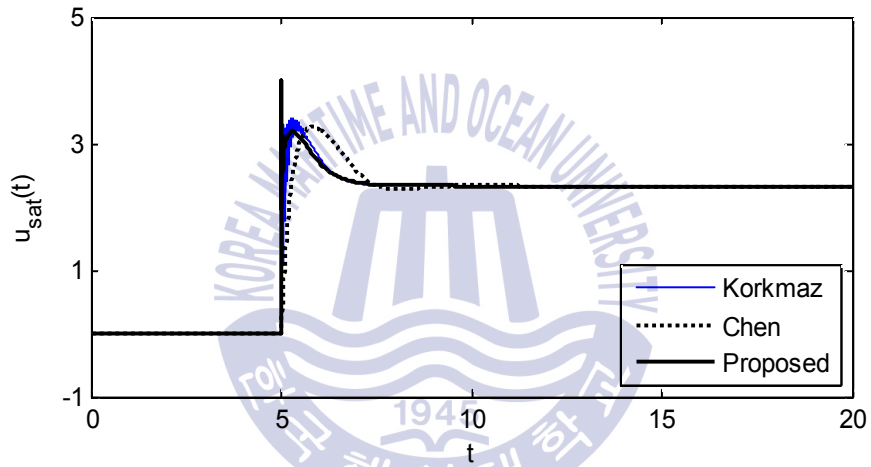
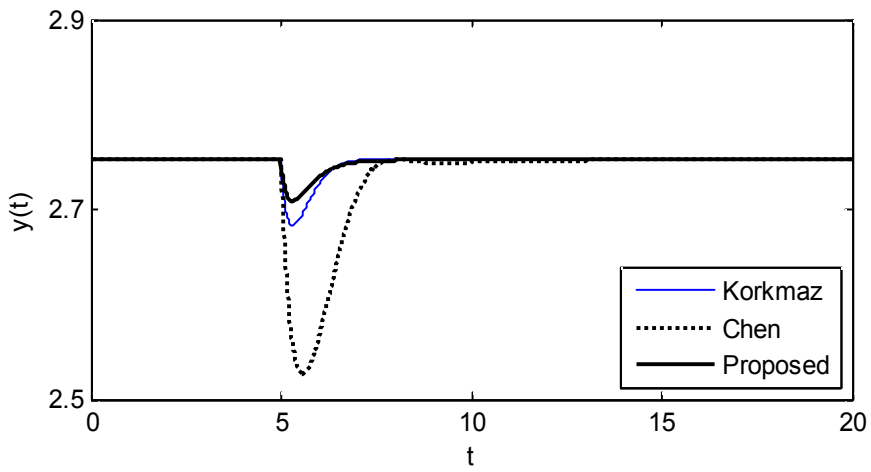


Fig. 5.7 Response comparison to parameter changes ($D_a = 0.072 \rightarrow 0.05$)

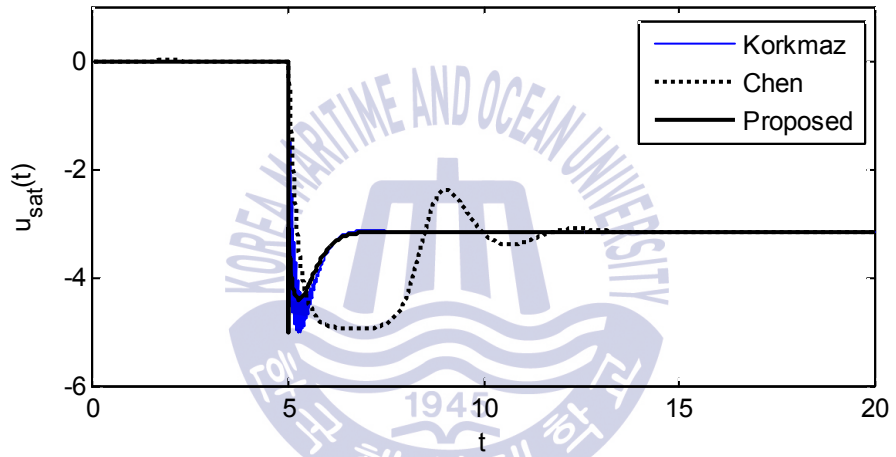
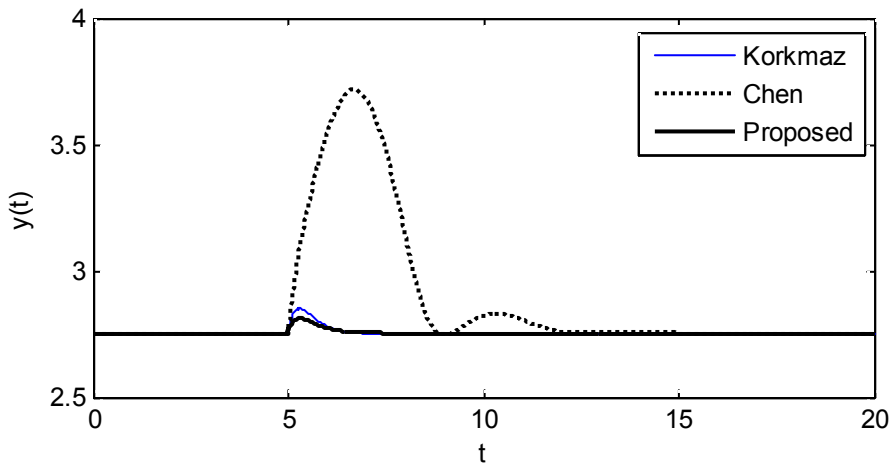


Fig. 5.8 Response comparison to parameter changes ($D_a = 0.09$, $H = 9$)

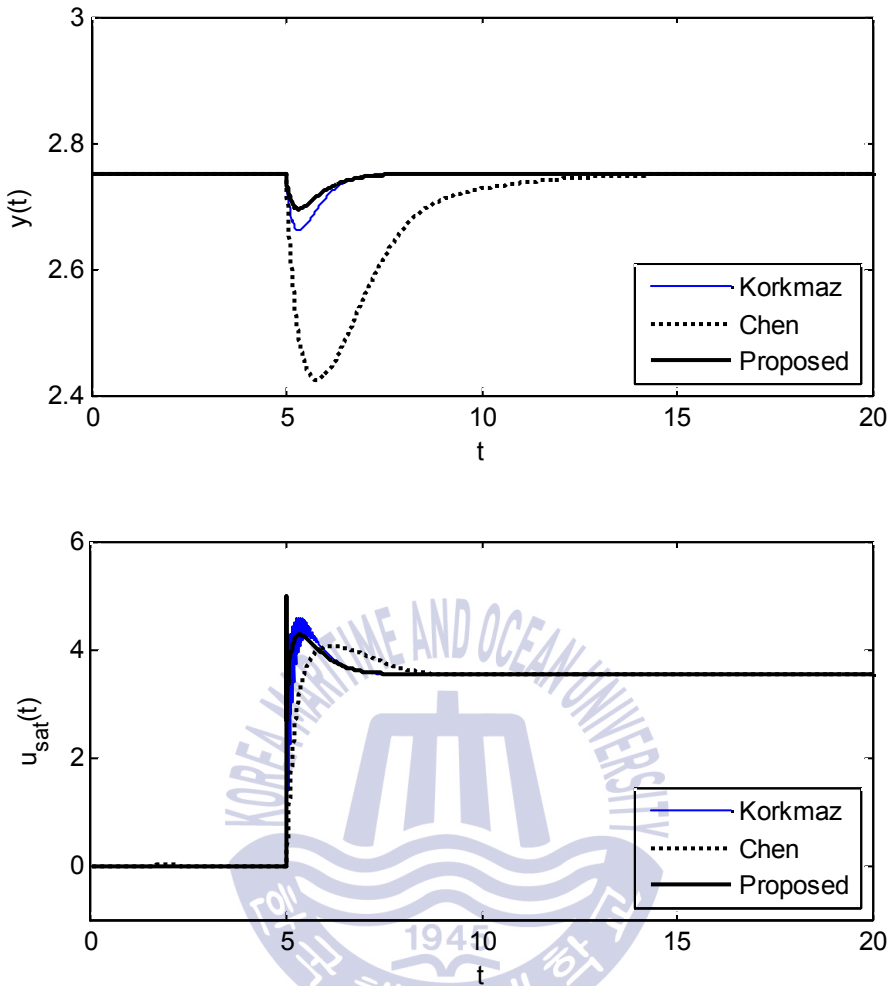


Fig. 5.9 Response comparison to parameter changes ($D_a = 0.05$, $H = 7$)

From these four simulation works, it can be found that the proposed controller and Korkmaz's controller are less sensitive to parameter changes, but the Chen's controller has unsatisfactory overall performance due to bigger peak value and longer recovery time if compared with the other methods. This can also be confirmed in Table 5.5 which shows quantitative results.

Table 5.5 Comparison of robustness to step-wisely parameter changes

Method	$D_a = 0.072 \rightarrow 0.09$				$D_a = 0.072 \rightarrow 0.09, H = 8 \rightarrow 9$			
	t_{peak}	M_{peak}	t_{rcy}	IAE	t_{peak}	M_{peak}	t_{rcy}	IAE
Proposed	0.30	0.03	1.79	0.03	0.32	0.06	2.86	0.06
Korkmaz	0.30	0.06	2.28	0.04	0.32	0.10	1.91	0.08
Chen	0.51	0.20	3.68	0.20	1.71	0.97	6.64	2.36

Table 5.6 Comparison of robustness to step-wisely parameter changes

Method	$D_a = 0.072 \rightarrow 0.05$				$D_a = 0.072 \rightarrow 0.05, H = 8 \rightarrow 7$			
	t_{peak}	M_{peak}	t_{rcy}	IAE	t_{peak}	M_{peak}	t_{rcy}	IAE
Proposed	0.33	0.04	2.43	0.04	0.35	0.06	3.15	0.06
Korkmaz	0.32	0.07	1.86	0.06	0.34	0.09	2.45	0.09
Chen	0.59	0.23	2.58	0.31	0.80	0.33	7.69	0.81

5.2.4. Comparison of computing time

As shown in Chapter 3, the Korkmaz's NPID controller has disadvantage of performing integral continuously at each control loop due to the use of the Gaussian error function as a nonlinear function. Integration can be performed by the trapezoidal method or the Simpson method, but the use of the NPID controller may be impossible due to the limit of computing time if it is implemented in a microprocessor.

Therefore, in this work, we has proposed a nonlinear gain function with better simplicity and performance in order to enhance the Korkmaz's NPID controller. To compare simple computing time between these two methods, programming was performed by using MATLAB and 500 times of repetitive executions were performed and averaged. It can be seen in Table 5.7 that the proposed method can save more time than the Korkmaz's method.

Table 5.7 Comparison of computation time

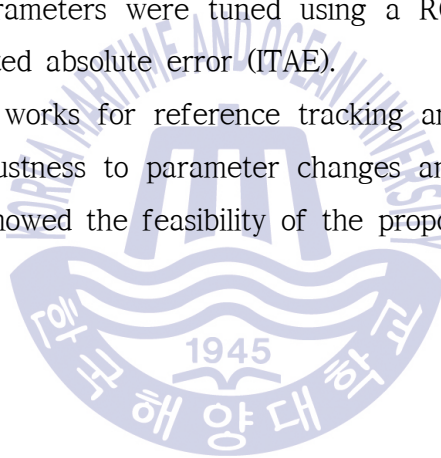
Methods	Computation time[msec]	Remarks
Proposed	0.3463	Intel(R) Core(TM)2 Duo CPU 3.00GHz Windows 7(32bits)
Korkmaz	34.4842	



Chapter 6. Conclusion

This thesis has presented a scheme of designing a nonlinear PID controller incorporating with a real-coded genetic algorithm (RCGA) for the temperature control of a CSTR process. The gains of the NPID controller were composed of easily implementable nonlinear functions based on the error and/or the error rate and its parameters were tuned using a RCGA by minimizing the integral of time-weighted absolute error (ITAE).

A set of simulation works for reference tracking and disturbance rejecting performances and robustness to parameter changes and comparison with two nonlinear controllers showed the feasibility of the proposed method.



References

- [1] W. H. Ray, *Advanced Process Control*, McGraw-Hill Book Co., N.Y., 1981.
- [2] J. P. Corriou, *Process Control: Theory and Applications*, Springer-Verlag, London, 2004.
- [3] B. W. Bequette, *Process Control: Modeling, Design, and Simulation*, Prentice Hall, 2002.
- [4] C. L. Smith, *Practical Process Control Tuning And Troubleshooting*, Wiley, 2009.
- [5] W. L. Luyben, *Process Modeling, Simulation and Control for Chemical Engineers*, McGraw-Hill Higher Education, 1989.
- [6] U. S. Banu and G. Uma, "Fuzzy Gain Scheduled Pole Placement Based on State Feedback Control of CSTR," *IET UK Int. Conf. on Information and Communication Technology in Electrical Sciences (ICTES 2007)*, India, pp. 63-68, 2007.
- [7] Geetha. M, Balajee. K.A and Jovitha Jerome, "Optimal Tuning of Virtual Feedback PID Controller for a Continuous Stirred Tank Reactor (CSTR) using Particle Swarm Optimization (PSO) Algorithm," *IEEE Int. Conf. on Advances in Engineering, Science and Management (ICAESM-2012)*, pp. 94-99, 2012.
- [8] F. Aslam and G. Kaur, "Comparative Analysis of Conventional, P, PI, PID and Fuzzy Logic Controllers for the Efficient Control of Concentration in CSTR," *Int. Journal of Computer Applications*, vol. 17, no.8, pp. 12-16, 2011
- [9] U. S. Banu and G. Uma, "Fuzzy Gain Scheduled CSTR with GA-Based PID," *Chem. Eng. Comm.*, vol. 195, pp. 1213-1226, 2008.

- [10] M. A. Nekoui, M. A. Khameneh and M. H. Kazemi, "Optimal Design of PID Controller for a CSTR System Using Particle Swarm Optimization(PSO)," *14th Int. Power Electronics and Motion Control Conference, EPE-PEMC 2010*, Ohrid, Republic of Macedonia, pp. T7-63-66, 2010.
- [11] C. T. Chen and S. T. Peng, "Learning Control of Process Systems with Hard Input Constraints," *J. of Process Control*, vol. 9, pp. 151-160, 1999.
- [12] L. S. Saoud, F. Rahmoune, V. Tourtchine and K. Baddari, "An Inexpensive Embedded Electronic Continuous Stirred Tank Reactor(CSTR) Based on Neural Networks," *2011 Int. Conf. on Multimedia Technology(ICMT)*, China, pp. 6233-6237, 2011.
- [13] Ziegler J. G. and N. B. Nichols, "Optimal Settings for Automatic Controllers." *Trans. ASME*, 64, 759-768, 1942.
- [14] K. J. Åström, and T. Hägglund, *PID Controllers: theory, design and tuning*, ISA Press, 1995.
- [15] M. Korkmaz, O. Aydogdu, and H. Dogan, "Design and performance comparison of variable parameter nonlinear PID controller and genetic algorithm based PID controller," *Proc. of 2012 IEEE Int. Symp. on Innovations in Intelligent Systems and Applications (INISTA)*, pp. 1-5, 2012.
- [16] O. Aydogdu and M. Korkmaz, "A Simple Approach to Design of Variable Parameter Nonlinear PID Controller," *2011 First Int. Conf. on Advancements in Information Technology, IPCSIT*, vol.20, pp. 81-85, Singapore, 2011.
- [17] Y. Li, G. Guo and Y. Wang, "A Nonlinear Control Scheme for Fast Settling in Hard Disk Drives," *IEEE Transactions on Magnetics*, vol. 40, no. 4, pp. 2086-2088, 2004.
- [18] J. Chen, B. Lu et al., "A Nonlinear PID Controller for Electro-Hydraulic Servo System Based on PSO Algorithm," *Applied Mechanics and Materials*, vol. 141, pp. 157-161, 2011.
- [19] G. So, M. So and G. Jin, "Design of a Nonlinear PID controller Based on

an Evolutionary Algorithm” , *2013 Conf. on Korea Society of Maritime Engineering*, pp. 374-374, Jinhae, 2013.

[20] G. Jin, *Genetic Algorithms and Their Applications*, Kyowoo Publishing Co., 2000.

